SLAC-PUB--5105

DE90 004429

MONITOR AND CONTROL SYSTEMS FOR THE SLD CHERENKOV RING IMAGING DETECTOR*

P. ANTILOGUS, D. ASTON, T. BIENZ, F. BIRD, S. DASU, W. DUNWOODIE, F. FERNANDEZ, G. HALLEWELL, H. KAWAHARA, P. KORFF, Y. KWON, D. LEITH, D. MULLER, T. NAGAMINE, T. PAVEL, L. RABINOWITZ, B. RATCLIFF, P. RENSING, D. SCHULTZ, S. SHAPIRO, C. SIMOPOULOS, E. SOLODOV+, N. TOGE, J. VAVRA, and S. WILLIAMS
Stanford Linear Accelerator Center, Stanford University, Stanford, CA 94309, USA

J. WHITAKER and R.J. WILSON
Boston University, Boston, MA02215, USA

A. BEAN, D. CALDWELL, J. DUBOSCQ, J. HUBER, A. LU, S. MCHUGH, L. MATHYS, R. MORRISON M. WITHERELL, and S. YELLIN
University of California, Department of Physics, Santa Barbara, CA 93106, USA

M. CAVALLI-SFORZA, P. COYLE, D. COYNE, P. GAGNON, D.A. WILLIAMS, and P. ZUCCHELLI**
Santa Cruz Institute for Particle Physics, University of California, Santa Cruz, CA 95064, USA

S. ATTANAGODA, R. JOHNSON, J. MARTINEZ, B. MEADOWS, M. NUSSBAUM, A. SHOUP, M. SOKOLOFF, and I. STOCKDALE
University of Cincinnati, Department of Physics, Cincinnati, OH 45221, USA

R. PLANO, P. JACQUES, and P. STAMER
Rutgers University, Serin Physics Laboratory Piscataway, NJ 08855, USA

K. ABE, K. HASEGAWA, F. SUEKANE, and H. YUTA
Tohoku University, Department of Physics, Aramaki, Sendai 980, Japan

Abstract

To help ensure the stable long-term operation of a Cherenkov Ring Imaging Detector at high efficiency, a comprehensive monitor and control system is being developed. This system will continuously monitor and maintain the correct operating temperatures, and will provide an on-line monitor of the pressures, flows, mixing, and purity of the various fluids. In addition the velocities and trajectories of Cherenkov photoelectrons drifting within the imaging chambers will be measured using a pulsed UV lamp and a fiberoptic light injection system.

Presented at the Accelerator Control: International Conference on Accelerator and Large Experimental Physics Control Systems, Vancouver, Canada, October 30–November 3, 1989.

* Work supported by Department of Energy contracts DE–AC03–76SF00515 and DE–AT03–79ER70023, and by the National Science Foundation under Grants PHY85–12145 and PHY85–13808.

+ Permanent Address: Institute of Nuclear Physics, Novosibirsk 630090, USSR.
** Present Address: Instituto di Fisica, Universita di Ferrara, I–44100 Ferrara, Italy.

CONF-891094--6

1. Introduction

A large Cherenkov Ring Imaging Detector (CRID) is currently under construction for the SLD detector [1,2] at the SLAC linear collider (SLC). This detector is designed to provide almost complete particle identification over 90% of the solid angle at the SLC, using barrel and endcap segments. By making use of both liquid (perfluoro-n-hexane, C_6F_{14}; $n = 1.227$ at $\lambda = 200$ nm) and gaseous (perfluoro-n-pentane, C_5F_{12}; $n = 1.0017$ at $\lambda = 200$ nm) radiators, $\pi/K/p$ separation will be possible up to about 30 GeV/c and e/π separation up to about 6 GeV/c.

Within the barrel CRID, Cherenkov photons are directed onto the quartz (fused silica) windows on the top and bottom of the drift tubes. The photons ionize the atmospheric-pressure drift gas which contains about 0.1% TMAE (tetrakis[dimethyl-amino]ethylene). The photoelectrons drift up to 1.27 m in a uniform electric field of about 400 V/cm and are detected at proportional wire planes.

Although CRID/RICH detection principles have been convincingly demonstrated in prototype studies by a number of groups [3,4], the main body of operational experience with large-scale TMAE-filled RICH detectors [5] has shown that such complex devices, which combine elements from many diverse technologies, require extensive on-line monitor and control systems [6] for stable long-term operation to be achievable.

2. Data acquisition

The monitor and control system is based on a parallel CAMAC[a] branch (fig. 1) supported by a DEC Vax station 3200. The workstation is one of several in the SLD cluster and is connected to the main SLD Vax 8800 via ethernet.

In general, the action of the computer and CAMAC is confined mainly to monitor, rather than direct control, functions. For example, the control of pressure in the CRID drift tube and radiator gas circuits — on which the integrity of the quartz windows depends — is accomplished using both an analog feedback system and firmware contained in a custom digital processor (§4.2).

The computer will, however, play a more active role in temperature control, where the large thermal inertia of the CRID should prevent rapid temperature fluctuations.

3. Monitor and control of operating temperature

Since a potentially damaging pressure differential might occur across the quartz windows of the drift tubes in the event of condensation of the C_5F_{12} radiator gas, the CRID vessel will be maintained at 40°C (±1°C), a safe margin above the C_5F_{12} condensation point of 30°C at 1 atm. The surfaces of the CRID vessel are populated

(a) Model 2922 Q-Bus-CAMAC interface with DMA and Model 3922 parallel branch crate controller: Kinetic Systems Corp., Lockport, IL 60441, USA.

with an array of Kapton-insulated heater pads and temperature sensors.[b] Heater power (15 KW at 150 V dc) is divided between "distributed" circuits whose pads are scattered in a regular geometric pattern over the whole surface of the vessel to provide uniform background heat, and "local" circuits whose pads are grouped together to provide local trim.

In the barrel CRID, approximately 200 heater circuits will provide a high level of redundancy. Approximately 50% of the available heater power will be provided by a backup diesel generator in the event of failure of the commercial electricity supply. The CAMAC-based temperature control system activates heater circuits based on the temperatures monitored by nearby sensors. A software database stores the required set points and the geometric correlation between the sensor positions and heater pads. In the event of a heater circuit failure, the software automatically switches control to the remaining circuits by increasing their 'on-time' duty cycle. A failed temperature sensor is automatically dropped from the active list from which heater operations are determined.

The current to each heater circuit is digitally switched using an individual ac "Zero-Crossing" solid state relay (SSR).[c] Switching operations are requested from software via a CAMAC output register.[d] The SSR is followed by a rectifier and a smoothing capacitor to provide "soft-start" DC current for use inside the SLD magnetic field. The voltage drop across a 3-Ohm series resistor is read by a CAMAC input register[e] as a check of circuit integrity.

The temperature sensor readout scheme utilizes up to 1024 inexpensive AD590JF sensors, multiplexed in 32-channel addresses into a CAMAC scanning ADC[f] using an "IDOM". AD590 sensors are chosen for their linear current output (nominally 1 μA/deg K). All sensors are calibrated at 40°C before installation, and in the more critical applications (usually those surfaces in contact with CRID fluids) each address is populated with 32 sensors sharing a tight common calibration (within ± 0.5°C of 40°C), connected to a single trim resistor on which the current output is converted to the monitor voltage. In less critical areas, sensors with a looser calibration are employed.

4. The CRID gas delivery and pressure control system

The barrel CRID gas supply and pressure control system is shown schematically in fig. 2.

(b) AD590: Analog Devices, Norwood, MA 02062, USA.

(c) 70 OAC5: Grayhill Inc., LaGrange IL 60525, USA.

(d) "IDOM" [Isolated Digital Output Module] 32 channels; J. Kieffer, SLAC Tech. Note 83–03.

(e) "IDIM" [Isolated Digital Input Module] 32 channels; J. Kieffer, SLAC Tech. Note 83–01.

(f) Kinetic Systems model 3527 Analog Input Module; see also D. Nelson, SLAC–ELD–DOC 39 (1983).

The base drift gas — ethane (C_2H_6) — is delivered through a Mass Flow Controller (MFC)[g] at atmospheric pressure and is bubbled through liquid TMAE maintained at a temperature of 28°C to pick up about 1 Torr of TMAE vapor. All gas piping between the TMAE bubbler and the drift tubes is maintained above 28°C to prevent recondensation of the TMAE vapor. The exhausts of the 40 drift tubes are monitored individually (§5).

The side walls of the drift tubes are of a two-layer construction with a purge space between the layers, which will be continuously flushed with pure methane (CH_4), supplied by a MFC. Although leak communication between the highly electronegative radiator gas and the TMAE-laden UV-absorbing drift gas through the two series glue joints is expected to be minimal, the sidewall exhaust gas will be monitored for evidence of leakage in either direction (§5).

Due to its expense, the C_5F_{12} radiator gas is continuously recirculated through the radiator vessel and a filter stack via a large turbine blower and MFC. Prior to filling with C_5F_{12}, the radiator vessel is purged of air by nitrogen (N_2) which is then thermodynamically replaced by C_5F_{12} using a refrigeration system. The density of the radiator gas will be monitored at several points using a sonar device [7] to determine the level of residual N_2 and any N_2/C_5F_{12} hydrostatic stratification. This technique is a simple alternative to the difficult direct measurement of refractive index in the UV to determine the effective Cherenkov thresholds.

To minimize the mechanical stress on the fragile CRID drift tubes, the differential pressure across the quartz windows is controlled with a triple-layered safety system:

(1) In normal operation analog feedback from sensitive pressure transducers to the delivery MFC's will maintain the correct differential pressures by regulating the flow of the input gases;

(2) Outside the normal operating ranges, signals from pressure sensors are used in a custom processor to sequentially open or close a series of input flow and overpressure or underpressure relief valves;

(3) In the event of failure of both electronic systems, a bi-directional passive pressure relief bubbler allows excess gas to leave the radiator vessel in the event of an overpressure, or admits air in the event of an underpressure.

Figure 3 illustrates the envelope of operation of the three systems.

4.1. The analog pressure control system

Sensitive electronic pressure sensors[h] monitor the pressure between the radiator vessel and atmosphere, between the drift tube sidewall purge inputs and

---

(g) Model 258B; MKS Inc., Burlington, MA 01803, USA.

(h) MKS Model 262 Capacitance Manometer: ±10 Torr full scale.

atmosphere, and between the radiator and drift gas inputs. Analog voltage signals (A, B, and C, respectively, in fig. 2) from these sensors are fed back to the MFC electronic controllers[i] to regulate the input flow on the basis of the sensed pressure. Two sensors are mounted in parallel in each location, so that on failure of a single sensor, the control can be transferred to the survivor.

4.2. The custom pressure control processor

A custom digital processor [8] has been constructed to monitor the outputs of all the pressure sensors, and in response to pressure variations outside the allowed limits, to sequence the opening and closing of the various input, output, overpressure, and underpressure relief valves shown in fig. 2.

The system consists of four elements:

(1) *Comparator cards:* These compare the sensed pressures with operating range set points, (fig. 4; four for each sensor), and pass a four-bit comparator output word for each sensor to the pressure controller card;

(2) *The Pressure Control Card (PCC):* This contains a programmable logic IC[j] in which the sequenced valve response to the current pressure status of the system is programmed as a finite state machine. Figure 4 shows the 25-element response matrix for correlated variations in differential pressure between the drift and radiator gas circuits, and between the CRID radiator vessel and atmospheric pressure. The normal operating state is at the center of the matrix, where the pressure of the drift gas is between 0 and 1 Torr higher than the radiator gas, which is itself between 0 and 1 Torr higher than the atmospheric pressure.

Away from the normal state, the program opens and shuts valves in a sequence most likely to bring the system back to the normal state: In general, when a gas stream is shut off, the most upstream valve (at the highest pressure) is closed first, followed by valves further downstream. When the flow is re-established, the upstream valve is opened last. In most programmed steps only one valve is operated at a time. The PCC uses a slow 1 Hz clock whose frequency is matched to the typical valve actuation time.

(3) *The valves and valve driver cards.* All the remote-controlled shut-off valves are pneumatically actuated with compressed air switched by miniature solenoid valves [k] which operate with 5 V dc TTL logic with a power dissipation of 0.5 W per valve. Each shut-off valve is also equipped with a stem position-sensing microswitch. The valve driver circuit actuates valves in the combination selected by the pressure control card, and checks for the correct combination of valve stem position and the status of the drive voltage to the solenoid actuator for every valve. If an illegal combination occurs, indicating a solenoid or valve failure, an individual fault signal is passed back to the

[i] MKS model 260.
[j] EP1800: Altera Inc, Santa Clara 95051, USA.
[k] K3P02LO: Honeywell, Skinner Valve Division, New Britain, CT 06051, USA.

PCC which closes all the valves in the pressure control system and warns the operator.

(4) *The Uninterruptable Power (UPS) and Compressed Air Supplies.* Both the analog pressure control system and the processor are powered directly from high-capacity batteries using a 117 V ac charger on automatic changeover between the commercial electricity supply and a Diesel generator. Should both power systems fail, the low-power solenoid valves should assure operation of the system for several hours. Even after discharge of the batteries, or failure of the compressed air supply — which is itself backed up with a Diesel compressor — the system should shut down in an intrinsically safe state with all critical valves closed.

5. The general CRID fluid monitoring system

Figure 5 is a schematic of the barrel CRID gas monitoring system. The monitor actions are separated into sample selections and instrument selections, and are highly automated; the valve sequencing is controlled by a second ALTERA EP1800-based processor and valve driver cards. One selection manifold handles non-TMAE gas streams (the base drift gas and the radiator input and output gas) while the other selects among all streams that might contain TMAE (the gas leaving the TMAE bubblers, the individual drift tube outputs and sidewall purge exhaust). This functional separation is necessary due to the reactivity of TMAE which is incompatible with many types of elastomeric valve seals: the valves in the TMAE circuits are entirely of a stainless steel seat/bellows construction. It is clear that only one stream may be allowed into the selection manifold at a time. The selection manifolds must also be purged with nitrogen before successive samples, and some of the longer sample lines, are kept continuously passivated with nitrogen when not in use. The individual drift tube exhausts are self-passivating; the monitor lines originate from tee's at their separate exhaust bubblers.

Most instruments in the monitor system can be selected simultaneously. Gas from the non-TMAE manifold may be passed into a custom CAMAC sonar binary gas mixture analyzer [7], trace oxygen and water vapor monitors and a UV gas transmission monitor consisting of a deuterium lamp, grating monochromator gas cell, and wavelength-shifted photomultipliers. Wavelengths are selected with a CAMAC-controlled stepper motor, and transparency measurements are made over the entire CRID UV detection bandwidth (160–240 nm) with a custom CAMAC scaler module. Even the presence of trace levels of contamination (a few parts per million) of oxygen, water vapor, or ethylene (which strongly absorb UV) can seriously degrade CRID performance. Sample gases from the TMAE bubblers and drift tubes may be passed into a second cell where UV transmission measurement can reveal the concentration of TMAE vapor present.

In the drift tubes, the lifetime of drifting photoelectrons is particularly sensitive to the presence of electronegative contaminantion from leaks or impurities in the base gas or its TMAE dopant. As an example, in ethane — at a drift field of 400 V/cm — an electron lifetime of 150 μm would assure the transmission of only 87% of the photoelectrons over the maximum drift distance of 127 cm. We have developed an on-line "Electron Lifetime Monitor" (ELM; [9]): A miniature drift chamber containing a small

^{241}Am source that ionizes the TMAE-laden gas entering it. By varying the electrode voltages in the ELM with a CAMAC-interfaced HV power supply, the electron drift velocity and drift time can be varied. Pulse height data accumulated in a CAMAC multichannel analyzer are plotted *vs.* drift time to yield the lifetime of electrons drifting in the particular gas stream.

6. Monitoring of photoelectron drift

Accurate reconstruction of the coordinates of the incident Cherenkov photons requires current knowledge of the velocity (temperature- and pressure-dependent) and trajectories (influenced by the uniformity of the drift field, and the electrostatic effects of drifting positive ions and collected charges on the inner surfaces of the drift tubes) of the drifting photoelectrons. As an on-line monitor of these parameters, light from a pulsed UV flashlamp or a nitrogen laser will be injected into each drift tube at 19 fiducial positions through silica optical fibers[l] (fig. 6). A single 600 μm core silica/silica fiber[m] will transmit UV light from the source to a custom bulkhead fiber connector and 19-way splitter on each drift tube (fig. 6). At each end of the barrel CRID a bundle of 20 such fibers is gathered together at the focal point of the source.

Since the light division at each splitter is not uniform, the light output from each fiber is tuned with a simple tubular collimator which also serves to give a light spot less than 1 mm diameter at the quartz window.

Acknowledgements

The assistance of the engineering and technical staffs at the collaborating institutions is gratefully acknowledged.

(l) "Superguide G" SFS 200Z fiber: 200 μm silica core/silica cladding, Fiberguide Industries, Stirling NJ 07980, USA.

(m) "Superguide G" SFS 600Z.

References

[1] SLD Design Report, SLAC–273; UC–34D (May 1984).

[2] D. Aston et al, SLAC–PUB–4795 (June 1989); To be published in *Nucl. Instr. and Meth. A.*

[3] V. Ashford et al, SLAC–PUB–4118; *IEEE Trans. Nucl. Sci.*, **NS–34** (1987) 499.

[4] See for example: R. Arnold et al, CRN/HE 87–08; *Nucl. Instr. and Meth.* **A270** (1988) 255;
L. Eek et al, CERN EP/84–25; *IEEE Trans. Nucl Sci.*, **NS–31** (1984) 949.

[5] R. Apsimon et al, *IEEE Trans. Nucl. Sci.*, **NS–33** (1986)122; *ibid.* **NS–34** (1987) 504.

[6] G. Hallewell, SLD Internal Note 151 (Feb. 1986).

[7] G. Hallewell et al, *Nucl. Instr. and Meth.* **A219** (1988) 213.

[8] G. Hallewell et al, CRID Internal Note No. 53 (Oct. 1988).

[9] M. Cavalli-Sforza, SLD CRID Internal Note 15 (1986).

Figure Captions

Fig. 1. The CAMAC monitor and control data acquisition system of the SLD CRID.

Fig. 2. Schematic of the barrel CRID gas delivery system, showing some of the components of the pressure control system.

Fig. 3. Desired gas system responses to variation in gas pressure.

Fig. 4. Response matrix to correlated variations in pressure between the drift gas and radiator gas circuits, and between the pressure of the CRID radiator vessel and the atmospheric pressure.

Fig. 5. Schematic of the barrel CRID gas monitor system.

Fig. 6. The UV source and fiberoptic light distribution system for the injection of fiducial light into each drift tube.

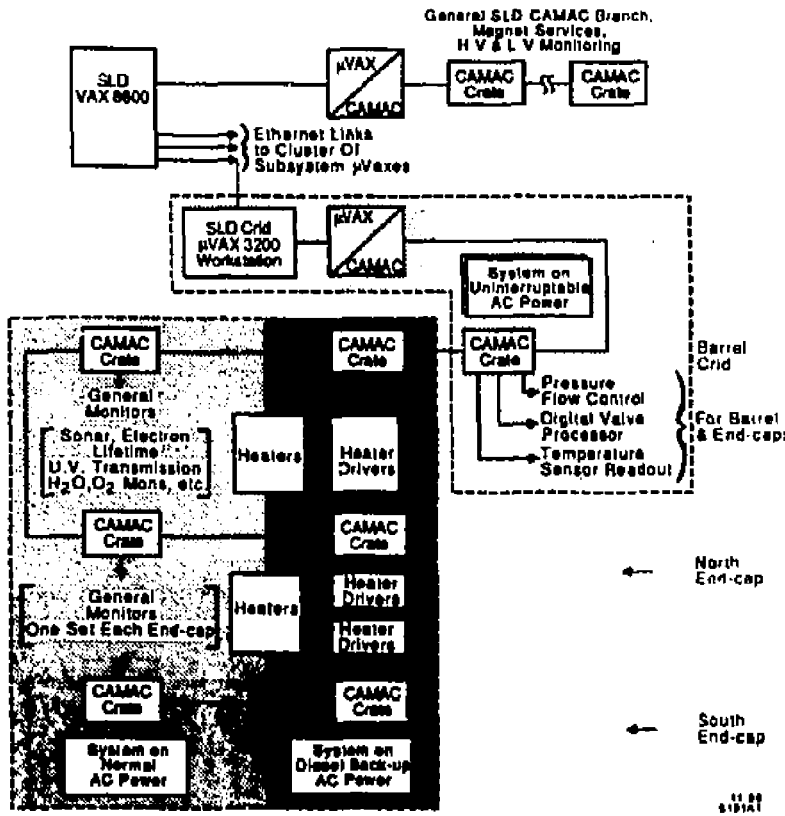
General SLD CAMAC Branch,
Magnet Services,
H V & L V Monitoring
SLD
VAX 8600
μVAX
CAMAC
CAMAC
Crate
CAMAC
Crate
Ethernet Links
to Cluster Of
Subsystem μVaxes
SLD Crid
μVAX 3200
Workstation
μVAX
CAMAC
System on
Uninterruptable
AC Power
CAMAC
Crate
CAMAC
Crate
Barrel
Crid
Pressure
Flow Control
Digital Valve
Processor
Temperature
Sensor Readout
For Barrel
& End-caps
CAMAC
Crate
General
Monitors
Sonar, Electron
Lifetime,
U.V. Transmission
H_2O,O_2 Mons, etc.
Heaters
Heater
Drivers
CAMAC
Crate
CAMAC
Crate
General
Monitors
One Set Each End-cap
Heaters
Heater
Drivers
Heater
Drivers
CAMAC
Crate
CAMAC
Crate
System on
Normal
AC Power
System on
Diesel Back-up
AC Power
North
End-cap
South
End-cap

Fig. 1

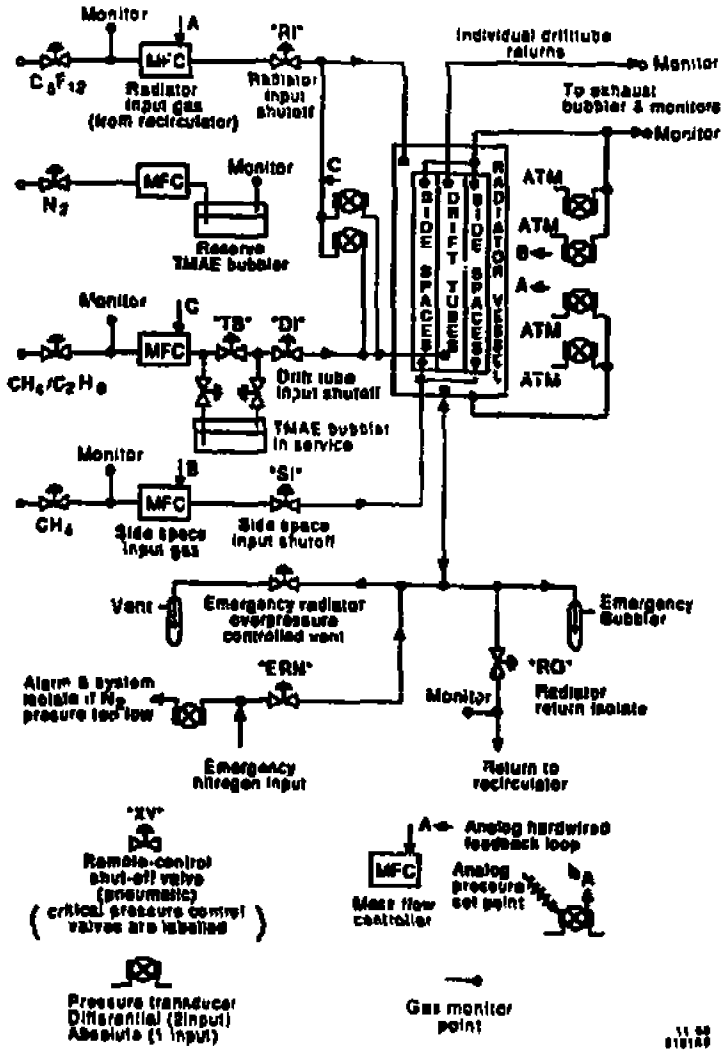
Monitor
A
MFC
"RI"
C_3F_{12}
Radiator input gas (from recirculator)
Radiator input shutoff
Individual drift tube returns
To Monitor
To exhaust bubbler & monitors
To Monitor
N_2
MFC
Monitor
C
Reserve TMAE bubbler
SIDE SPACE
DRIFT TUBES
SIDE SPACE
RADIATOR VESSEL
ATM
ATM
B
A
ATM
ATM
Monitor
C
MFC
"TB"
"DI"
CH_4/C_2H_6
Drift tube input shutoff
TMAE bubbler in service
Monitor
B
MFC
"SI"
CH_4
Side space input gas
Side space input shutoff
Vent
Emergency radiator overpressure controlled vent
Emergency bubbler
"ERM"
"RO"
Alarm & system isolate if N_2 pressure too low
Monitor
Radiator return isolate
Emergency nitrogen input
Return to recirculator
"XV"
Remote-control shut-off valve (pneumatic)
(critical pressure control valves are labelled)
A
Analog hardwired feedback loop
MFC
Mass flow controller
Analog pressure set point
A
Pressure transducer
Differential (2 input)
Absolute (1 input)
Gas monitor point

Fig. 2

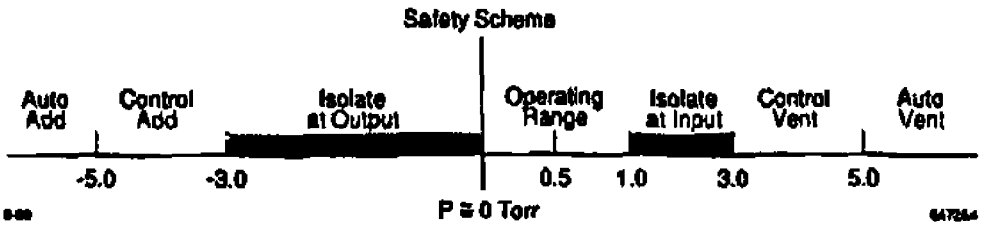
Safety Schema
Auto Add
Control Add
Isolate at Output
Operating Range
Isolate at Input
Control Vent
Auto Vent
-5.0
-3.0
0.5
1.0
3.0
5.0
P ≅ 0 Torr

Fig. 3

DIFFERENTIAL PRESSURE:
(DRIFT GAS - RADIATOR GAS : TORR)

-3	0	1	+3	
\DI \RI \RO ERN dGS | EN	\RI \RO ERN dNS | wEN	\RI \RO ERN dNS | wEN	\DI \RI \RO ERN dGS | wEN	\DI \RI \RO ERN dGS | wEN	-3
\DI \RO dGS | wRI	\RO dNS | wRI	\RO dNS | wRI	\DI \RO dGS | wRI	\DI \RI \RO ERN dGS | wEN	0
dNS | wNS	dNS | wNS	NIRVANA dNS | wNS	\DI dGS | wNS	\DI dGS | wNS	+1
\DI \RI \RO ERV dGS | wEV	\RI dNS | wRO	\RI dNS | wRO	\DI \RI dGS | wRO	\DI \RI dGS | wRO	+3
\DI \RI \RO ERV dGS | wEV	\RI \RO ERV dNS | wEV	\RI \RO ERV dNS | wEV	\DI \RI \RO ERV dGS | wEV	\DI \RI \RO ERV dGS | wEV	

DIFFERENTIAL PRESSURE (RADIATOR GAS - ATMOSPHERIC PRESSURE: TORR)

LEGEND

\DI	Drift Input Closed ($\overline{DIA,DIB}$)
\RI	Radiator Input closed ($\overline{RIA,RIB}$)
\RO	Radiator Output closed
ERV	Emergency Radiator Vent valve open
ERN	Emergency Radiator Nitrogen input open

Fig. 4

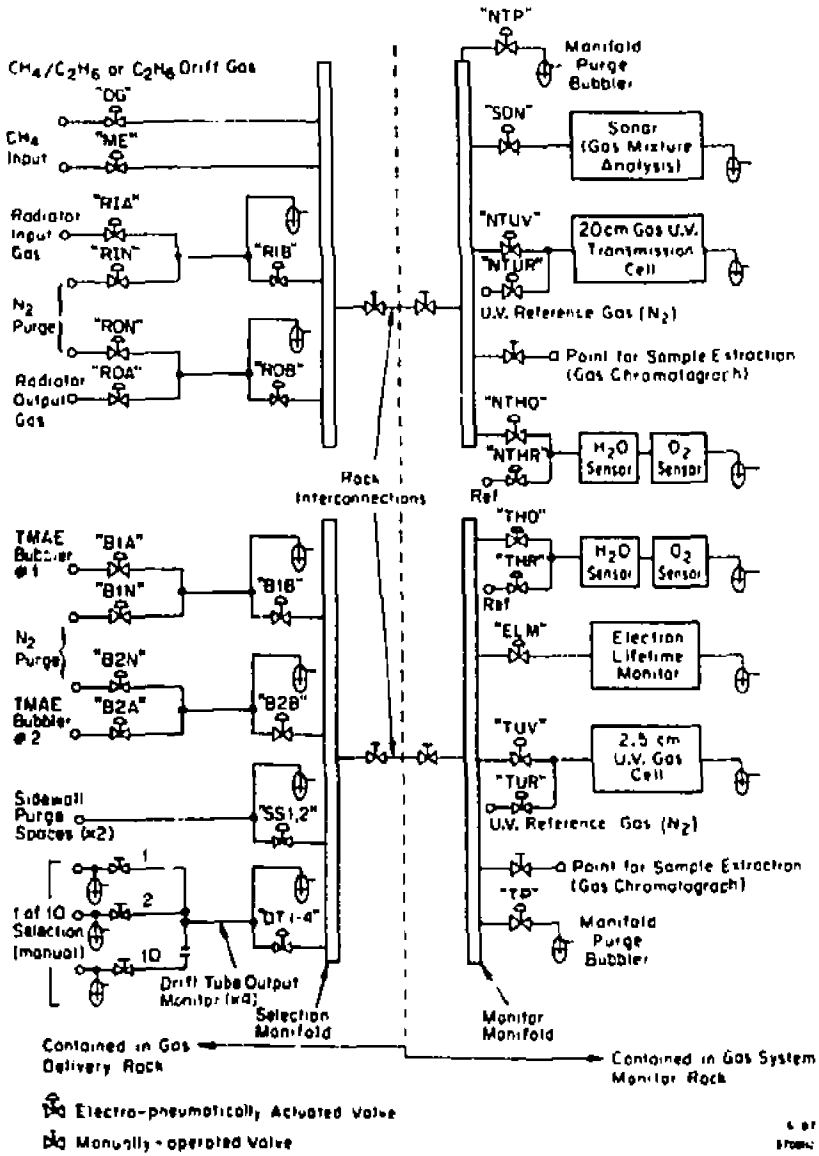
"NTP"
Manifold Purge Bubbler
CH_4/C_2H_6 or C_2H_6 Drift Gas
"DG"
CH_4 Input
"ME"
"SON"
Sonar (Gas Mixture Analysis)
"RIA"
Radiator Input Gas
"RIN"
"RIB"
"NTUV"
20cm Gas U.V. Transmission Cell
"NTUR"
N_2 Purge
"RON"
U.V. Reference Gas (N_2)
Point for Sample Extraction (Gas Chromatograph)
Radiator Output Gas
"ROA"
"ROB"
"NTHO"
"NTHR"
H_2O Sensor
O_2 Sensor
Rack Interconnections
Ref
"THO"
TMAE Bubbler #1
"B1A"
"B1N"
"B1B"
"THR"
H_2O Sensor
O_2 Sensor
Ref
N_2 Purge
"B2N"
"ELM"
Electron Lifetime Monitor
TMAE Bubbler #2
"B2A"
"B2B"
"TUV"
2.5 cm U.V. Gas Cell
"TUR"
Sidewall Purge Spaces (x2)
"SS1,2"
U.V. Reference Gas (N_2)
Point for Sample Extraction (Gas Chromatograph)
"TP"
1 of 10 Selection (manual)
"DT1-4"
Manifold Purge Bubbler
Drift Tube Output Monitor (x4)
Selection Manifold
Monitor Manifold
Contained in Gas Delivery Rack
Contained in Gas System Monitor Rack
Electro-pneumatically Activated Valve
Manually-operated Valve

Fig. 5

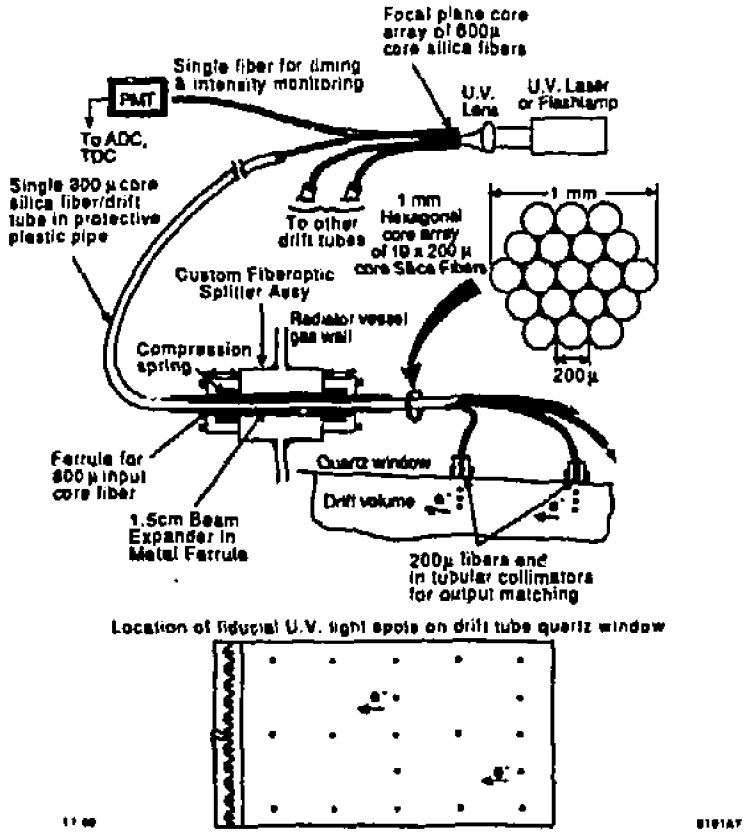
Focal plane core array of 600μ core silica fibers
Single fiber for timing & intensity monitoring
PMT
To ADC, TDC
U.V. Lens
U.V. Laser or Flashlamp
Single 800 μ core silica fiber/drift tube in protective plastic pipe
To other drift tubes
1 mm Hexagonal core array of 19 x 200 μ core Silica Fibers
1 mm
200μ
Custom Fiberoptic Splitter Assy
Radiator vessel gas wall
Compression spring
Ferrule for 800 μ input core fiber
1.5cm Beam Expander in Metal Ferrule
Quartz window
Drift volume
200μ fibers and in tubular collimators for output matching
Location of fiducial U.V. light spots on drift tube quartz window

Fig. 6